Research Article

Molecular Cancer Therapeutics

# Docetaxel-Resistant Prostate Cancer Cells Remain Sensitive to *S*-Trityl-L-Cysteine–Mediated Eg5 Inhibition

Carolyn Wiltshire[1,2], Babloo L. Singh[1,2], Jacqueline Stockley[4], Janis Fleming[2], Brendan Doyle[2], Robert Barnetson[3], Craig N. Robson[4], Frank Kozielski[2], and Hing Y. Leung[1,2]

## Abstract

Castrate-resistant prostate cancer remains a major clinical challenge. Due to the toxicity profile of taxane-based chemotherapy and treatment failure in some patients, novel agents with improved efficacy to side effect profiles are urgently needed. Eg5, a member of the kinesin-5 family, controls the formation of the bipolar spindle during cell division, and suppressed Eg5 function leads to mitotic arrest. *S*-Trityl-L-cysteine (STLC) is a novel Eg5-specific small-molecule inhibitor. Here, we report the first study to evaluate its use in prostate cancer. In a panel of prostate cancer cells, LNCaP and PC3 cells were the most and least sensitive to STLC treatment, with a 7.2-fold difference in their respective $GI_{50}$ values: 250 nmol/L and 1.8 μmol/L. In LNCaP cells, treatment with either STLC or docetaxel resulted in transient $G_2$-M arrest and subsequent caspase-mediated cell death. However, STLC- and docetaxel-treated PC3M cells have distinct fates: STLC induced a transient $G_2$-M arrest, followed by polyploidy; in contrast, docetaxel-treated PC3M cells progressed to apoptosis after a transient $G_2$-M arrest. Docetaxel-resistant LNCaP-derived (LDocR) cells respond to STLC in a similar manner to the parental cells. Although the docetaxel-resistant PC3M-derived (PDocR) cell line and its parental PC3M cells have similar $GI_{50}$ to STLC treatment, PDocR cells showed significantly more $G_2$-M arrest and less apoptosis. Hence, although docetaxel-resistant prostate cancer cells remain responsive to Eg5 inhibition with STLC, there are key differences at the cell cycle level, which may have implication in future development. *Mol Cancer Ther; 9(6); 1730–9. ©2010 AACR.*

## Introduction

Kinesins are a large superfamily of motor proteins that participate in multiple biological phenomena including mitosis and intracellular transport of vesicles and organelles (1). Kinesins consist of a long coiled-coil stalk with a cargo binding tail at one end and a globular motor domain, usually called the head, at the other. To date, there are at least 12 kinesins involved in mitosis and meiosis, which are responsible for spindle and chromosomal movement (2). Among them, Eg5 (or KSP) is a slow, plus-end–directed motor of the kinesin-5 subfamily (3). Eg5 forms a homotetrameric structure capable of binding antiparallel microtubules and sliding them apart. It acts during the early stages of mitosis and is responsible for centrosome separation and bipolar spindle assembly, which are essential for proper segregation of chromosomes (3). Failure of Eg5 function leads to cell cycle arrest in mitosis with monoastral microtubule arrays (3, 4). The important role of Eg5 in mitotic progression makes it an attractive candidate for developing targeted therapy in cancer.

Tubulin, a heterodimeric protein, plays an intrinsic role in cytoskeleton and mitotic spindle physiology. Microtubule-directed agents belong to the most successful anticancer agents. Besides its use in a wide range of tumor types, paclitaxel (Taxol) remains the only chemotherapy agent to have demonstrable survival benefit in (castrate-resistant) prostate cancer sufferers. Unfortunately, despite its significant toxicity profile, many patients' tumors develop resistance to Taxol. Agents that target mitotic kinesins, such as Eg5, selectively would be an appealing alternative. Eg5 inhibitors are expected to act on cells undergoing cell division and, hopefully, have fewer side effects than drugs inhibiting other essential microtubule-based processes. Several Eg5-specific inhibitors including *S*-trityl-L-cysteine (STLC) are currently optimized for their potential use in cancer chemotherapy (5). STLC (Fig. 1A) is a reversible, tight-binding inhibitor of Eg5, inducing prolonged mitotic arrest and subsequent apoptosis in cell lines derived from different tumor types (6–8). STLC is currently under further chemical optimization and the best analogues have $IC_{50}$ values *in vitro* and in cell-based assays in the low nanomolar range (6, 9, 10).

**Authors' Affiliations:** [1]Division of Cancer Sciences and Molecular Pathology, University of Glasgow; [2]Beatson Institute for Cancer Research; [3]Department of Pathology, NHS Greater Glasgow and Clyde, Glasgow, United Kingdom; and [4]Northern Institute for Cancer Research, Newcastle upon Tyne, United Kingdom

**Note:** Supplementary material for this article is available at Molecular Cancer Therapeutics Online (http://mct.aacrjournals.org/).

**Corresponding Author:** Hing Y. Leung, Beatson Institute for Cancer Research, Switchback Road, Bearsden, Glasgow G61 1BD, United Kingdom. Phone: 44-141-330-3658; Fax: 44-141-942-6521. E-mail: h.Leung@beatson.gla.ac.uk

**doi:** 10.1158/1535-7163.MCT-09-1103

©2010 American Association for Cancer Research.

Downloaded from http://aacrjournals.org/mct/article-pdf/9/6/1730/1888559/1730.pdf by guest on 20 September 2024

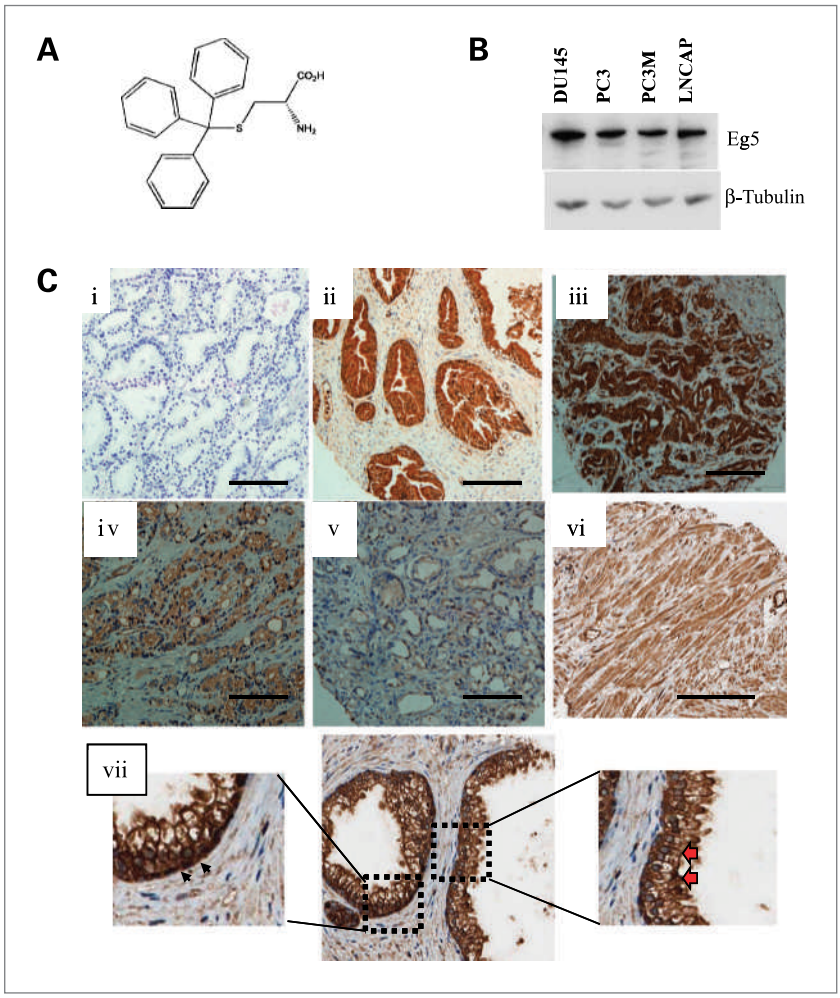


Figure 1. STLC treatment impairs growth in a panel of human prostate cancer cell lines. A, chemical structure of STLC. B, Western blot showing Eg5 expression in a panel of human prostate cancer cell lines. C, immunohistochemical staining for Eg5: i, negative control in a case of prostate cancer; ii and iii, strong cytoplasmic Eg5 staining in malignant epithelium; iv, moderate level of Eg5 expression in a cancer case; v, low level of Eg5 in a cancer case; vi, smooth muscle cells with moderate level of Eg5 expression; vii, Eg5 expression in a case of benign prostatic hyperplasia: cytoplasmic signal in basal cells (black arrows, left inset) and cytoplasmic/membranous signal in luminal cells (red arrows, right inset). The scale (black line) in images (i) to (vi) represents 100 μm; image (vii) was magnified to highlight the basal and luminal cells.

Here, we report for the first time the use of STLC, an Eg5-specific small-molecule inhibitor, in prostate cancer. The *in vitro* cellular responses following STLC treatment in human prostate cancer cells were examined, including the effects on mitotic arrest and cell death.

## Materials and Methods

### Cell culture

LNCaP, DU145, PC3, and PC3M cell lines were cultured and maintained in RPMI 1640 (Gibco BRL) supplemented with 1% L-glutamine and 10% FCS at 37°C in 5% $CO_2$. PC3M cells are a metastatic derivative of PC3 cells (11). Docetaxel-resistant derivatives of LNCaP and PC3M (LDocR and PDocR) were generated by continuous culture in increasing concentrations of docetaxel until they developed the ability to grow and divide in the presence of the drug. Parental prostate cancer LNCaP and PC3M cells were serially cultured for 5 months in the presence of increasing doses of docetaxel (from 0.1 to 2 nmol/L) until cells were able to survive and divide in the presence of 2 nmol/L docetaxel, at which point the cells were cryopreserved for future experiments. Derivative cell lines maintained in 2 nmol/L docetaxel were termed LDocR and PDocR, respectively. Similarly, an androgen-independent subline of LNCaP cells was derived by chronic androgen starvation in steroid-depleted medium over a period of 9 months. These cells were serially maintained in steroid-depleted medium and were termed LNCaP-AI. The $GI_{50}$ values for docetaxel are as follows: LNCaP, 1.63 nmol/L; PC3M, 6 nmol/L; LDocR, 22.4 nmol/L; PDocR, 21.2 nmol/L. These cells were maintained as for the parental cells but with 2 nmol/L docetaxel included in the growth medium. Docetaxel and STLC were supplied by Sigma and the National Cancer Institute, NIH, and stock solutions were prepared in DMSO.

### Cell proliferation assay

Assays were carried out using the WST-1 cell proliferation reagent (Roche) as per manufacturer's instructions. Cells were seeded into flat-bottomed 96-well plates at a density of 4,000 to 10,000 cells per well and allowed to attach for 24 hours, and then medium was replaced with fresh medium containing serial dilutions of drugs or

Downloaded from http://aacrjournals.org/mct/article-pdf/9/6/1730/1888559/1730.pdf by guest on 20 September 2024

DMSO alone. After 72 hours, WST-1 assay reagent was added, mixed, and left to develop for 4 hours before reading the absorbance at 450 and 650 nm on a Safire 2 Multilabel Microplate reader (Tecan). Results were corrected for cell-only controls. Data were averaged from duplicate experiments. $GI_{50}$ signifies the concentration of the test drug that causes 50% growth inhibition and is calculated as $100 \times (T - T_0)/(C - T_0) = 50$, where the absorbance of the test well at the end of experiment following exposure to test drug is $T$, the absorbance at time zero is $T_0$, and the control absorbance is $C$.

### Drug treatment for cell cycle profiling and preparation of cell extracts

Cells were seeded into 75-$mm^2$ flasks at a density of $1.5 \times 10^6$ to $3 \times 10^6$ per flask, in duplicate. After 24 hours, medium containing DMSO alone, docetaxel, or STLC was added to each flask, and this was considered the 0-hour time point. The doses of docetaxel and STLC used for parental cell lines were approximately 5-fold higher than the respective $GI_{50}$ doses (for LNCaP, 10 nmol/L docetaxel and 1 μmol/L STLC; for PC3M, 20 nmol/L docetaxel and 5 μmol/L STLC). STLC treatment in LNCaP and LDocR cells was administered at equipotent doses corresponding to the respective $GI_{80}$. The choice of docetaxel dose at 10 to 20 nmol/L for LNCaP and PC3M cells was based on an equipotent dose of docetaxel, which would produce a similar level of growth inhibition ($\sim GI_{80}$) to that used in STLC growth assays. Docetaxel was used at approximately the $GI_{50}$ dose in docetaxel-resistant variants (20 nmol/L for both cell types). For each time point, duplicate flasks were harvested by collecting all cells [both adhered (by trypsinization) and floating in medium] by centrifugation. After two PBS washes, samples for propidium iodide (PI) staining and cell cycle analysis were resuspended in 5 mL of ice-cold 70% ethanol and stored at 4°C for at least 1 hour before proceeding. Cell pellets for cell extract preparation were frozen on dry ice and stored at −80°C until required.

### Cell cycle analysis

Cells fixed in 70% ethanol were collected by centrifugation and rinsed twice in cold PBS. Cellular DNA was then stained in PBS containing 10 μg/mL PI and 10 μg/mL RNase A. Data were collected using CellQuest software on a FACSCalibur cytometer (BD Biosciences). Analysis and quantification were carried out using WinMDI 2.8 (The Scripps Research Institute, San Diego, CA). Percentages of cells in the different stages in the cell cycle were estimated from their DNA content [sub-$G_1$ (DNA < 2N), $G_2$-M (DNA = 4N), and polyploid (DNA > 4N)]. Figures on data from cell cycle analysis represent triplicate experiments.

### SDS-PAGE and Western blotting

Cell extracts were prepared by resuspending frozen pellets in a buffer containing 50 mmol/L Tris (pH 7.6), 150 mmol/L NaCl, 1% (v/v) Triton X-100, 0.5% (w/v) sodium deoxycholate, 0.1% (w/v) SDS, 1 mmol/L sodium orthovanadate, 5 mmol/L sodium fluoride, and 50 mmol/L phenylmethylsulfonyl fluoride containing 1× protease inhibitor cocktail I (Merck), allowing the cells to swell on ice before centrifugation at 10,000 rpm for 10 minutes. Lysates were transferred to fresh tubes and assayed for protein concentration. For Western blotting, 20 μg of total protein were denatured in 5× loading buffer (Fermentas), then resolved by SDS-PAGE on either 10% or 4–12% gradient NuPAGE Bis-Tris gels (Invitrogen) and immobilized on prewetted polyvinylidene difluoride membranes (Millipore). Membranes were blocked in TBS containing 0.1% Tween 20 (TBST) and 5% milk before incubation with primary antibodies diluted in TBST containing 5% bovine serum albumin. The antibody against β-tubulin (Sigma) was used at 1:2,000 dilution, whereas antibodies against phospho-$Thr_{232}$ Aurora B (Stressgen, Cambridge Bioscience), cyclin B1 (BD Pharmingen), PARP (Trevigen, AMS Biotechnology), and cleaved caspase-3 and caspase-7 (NEB) were used at 1:1,000. Subsequently, blots were incubated with relevant horseradish peroxidase–conjugated secondary antibodies (NEB) at a dilution of 1:5,000 and visualized using enhanced chemiluminescence (GE Healthcare Life Sciences).

### Eg5 expression by Western blot analysis and immunohistochemistry

Western blot and immunohistochemistry experiments were done as described previously (12). Tissue microarray of prostate cancer biopsies, consisting of $n = 24$ benign and 43 cancer specimens, was prepared with local ethical committee approval. Eg5-specific antibody (Cytoskeleton, Inc.) was optimized for Western blot and immmunostaining at 1:1,000 and 1:5,000 dilutions, respectively.

### MDR activity assay

MDR activity was measured by the calculation of rhodamine efflux from cells as previously described (13). Verapamil hydrochloride (Sigma) was used as an MDR1 inhibitor. Efflux was determined after 90 minutes following two washes with PBS, when the rhodamine content of the cells were examined using a Becton Dickinson FACScan. Cells with an increased activity of MDR1 showed a lower fluorescence on the FL1 channel at 37°C when compared with the biologically inactive 4°C sample, which was reversible in the presence of verapamil hydrochloride.

### Statistics

Graphs were plotted using Microsoft Excel, and data presented are the mean, with error bars signifying SE. Cell cycle analysis results for parental and docetaxel-resistant derivative lines were tested for statistical significance using a Student's $t$ test (95% confidence).

## Results

DU145 and PC3 cells express marginally more Eg5 than LNCaP and PC3M cells, with normalized ratios to the respective β-tubulin level at 0.9 for DU145 and PC3

Downloaded from http://aacrjournals.org/mct/article-pdf/9/6/1730/1888559/1730.pdf by guest on 20 September 2024

cells and 0.6 for LNCaP and PC3M (Fig. 1B). $GI_{50}$ values of STLC were summarized in Table 1. Consistent with the reported specificity of STLC in targeting Eg5, the formation of monastral spindles was observed in our prostate cancer cells (data not shown). Between the most and least sensitive (parental) prostate cancer cells, namely, LNCaP and PC3, there was a 7.2-fold difference in their respective $GI_{50}$ values (Table 1).

Using immunohistochemistry to study Eg5 expression in clinical prostate cancer tissue, we observed Eg5 immunoreactivity in both basal and luminal epithelial cells in benign prostatic hyperplasia, with cytoplasmic signal in the basal cells and membranous and cytoplasmic staining in the luminal cells. Smooth muscle cells also showed moderate cytoplasmic staining, with little or no stromal staining. Overall, there was no significant difference in Eg5 expression between benign and malignant prostate tissues (Fig. 1C; Mann-Whitney test, $P = 0.1$).

After 24 hours of exposure to STLC, 73.3% (±6%) of LNCaP cells and 87.3% (±3.1%) of PC3M cells had a DNA content representative of cells in the $G_2$-M phase of the cell cycle (Fig. 2A). In LNCaP cells, this population remained at a similar level at 72.9% (±0.9%) at 48 hours, before decreasing to 40.9% (±1.4%) at 72 hours. Blotting of matched extracts for the presence of biological hallmarks of the $G_2$-M transition, namely, cyclin B1 and phospho-$Thr_{232}$ Aurora B, confirmed that LNCaP cells arrested in $G_2$-M for the first 48 hours following STLC treatment (Fig. 2B). The level of PC3M cells in $G_2$-M had decreased by 10% to 77.2% (±2.3%) at 48 hours, being further reduced to 46.4% (±6.5%) at 72 hours (Fig. 2A). The presence of cyclin B1 and phospho-$Thr_{232}$ Aurora B at 24 hours but not at later time points confirmed that $G_2$-M arrest induced by STLC in PC3M was more transient than that in LNCaP cells, lasting only 24 hours as opposed to 48 hours. Interestingly, parallel comparative experiments with docetaxel treatment revealed a similar profile of $G_2$-M arrest in both LNCaP and PC3M cells.

**Table 1.** $GI_{50}$ values in a panel of prostate cancer cells including the docetaxel-resistant derived cell lines from LNCaP and PC3M cells

| Cell lines | $GI_{50}$ |
|---|---|
| LNCaP | 250 nmol/L |
| PC3 | 1.8 μmol/L |
| PC3M | 850 nmol/L |
| DU145 | 1.6 μmol/L |
| LNCaP-derived docetaxel-resistant (LDocR) cells | 200 nmol/L |
| PC3M-derived docetaxel-resistant (PDocR) cells | 820 nmol/L |
| LNCaP-derived androgen-independent (LNCaP-AI) cells | 400 nmol/L |

Hence, between PC3M and LNCaP cells, there seems to be a quantitative difference in mitotic arrest following treatment with STLC.

We observed a reduction in the LNCaP population in $G_2$-M arrest after 48 hours of treatment with either STLC or docetaxel. In addition, this was followed by an increase in cells with a sub-$G_1$ DNA content (Fig. 2A), increasing from 8.3% (±0.6%) at 48 hours to 21.1% (±1.7%) at 72 hours. This is consistent with the model that Eg5 inhibition induces apoptosis after prolonged mitotic arrest (the underlying mechanism of which remains not fully understood). Hence, protein lysates from matched samples were probed for active (cleaved) forms of executioner caspase-3, caspase-7, and cleaved PARP. Cleavage of all three proteins was observed after 48 and 72 hours of STLC treatment (Fig. 2B), consistent with a temporal relationship of mitotic arrest followed by apoptosis in LNCaP cells. Again, the response of LNCaP cells to docetaxel treatment was similar to that of STLC (Fig. 2B).

Contrary to the results in LNCaP cells, the proportion of PC3M cells with a sub-$G_1$ DNA content differs significantly following treatment with STLC or docetaxel (Fig. 2A and Supplementary Fig. S1). Whereas the portion of sub-$G_1$ cells increased in a time-dependent manner following docetaxel treatment [from 10.5% (±2.3%) at 24 hours to 20.5% (±2.5%) at 48 hours and 25.3% (±1.4%) at 72 hours], a more reduced sub-$G_1$ population was observed following STLC treatment [2% (±1%) at 24 hours to 5.8% (±1%) at 48 hours and 11.5% (±2.1%) at 72 hours]. Blotting also indicated that less of the cleaved forms of PARP, caspase-3, and caspase-7 were present in STLC-treated PC3M cells when compared with docetaxel treatment (Fig. 2B). Therefore, STLC-treated PC3M cells may be subjected to a different fate than docetaxel-treated cells. It has been reported previously that paclitaxel-treated PC3 cells undergo a rapid mitotic slippage after a transient mitotic arrest, resulting in the appearance of polyploidy cells through the process of endo-reduplication (14). Examination of the cell cycle profiles of STLC-treated PC3M cells indicated the presence of a population of cells with 8N DNA content (Fig. 2A). This was found to increase in a time-dependent manner from 9.5% (±2.4%) at 48 hours to 29.7% (±5.7%) at 72 hours. Whereas STLC-treated PC3M cells underwent a transient $G_2$-M arrest followed by polyploidy, docetaxel-treated PC3M cells progressed to apoptosis after a transient $G_2$-M arrest. Docetaxel treatment of PC3M cells resulted in a small proportion of polyploidy cells, which did not increase further with prolonged treatment up to 72 hours. In contrast, LNCaP cells did not become appreciably polyploidy with either treatment (Supplementary Fig. S1B). The difference in the responses of LNCaP and PC3M cells to STLC may be accounted for, in part, by their p53 status—PC3 (and therefore PC3M) cells are p53 deficient, whereas LNCaP contain proficient p53 (15). Because the polyploidy checkpoint is p53 dependent (16, 17), it would be expected that LNCaP would retain a functional checkpoint, triggering cells to undergo apoptosis, whereas PC3M may not.

Downloaded from http://aacrjournals.org/mct/article-pdf/9/6/1730/1888559/1730.pdf by guest on 20 September 2024

Docetaxel-resistant cells derived from LNCaP (LDocR) were tested for sensitivity to STLC in a cell proliferation assay and found to have a $GI_{50}$ of approximately 200 nmol/L, which is comparable to that of the parental cells (Table 1). Cell cycle profiling indicated that, as for the parental LNCaP cells, a high proportion of the LDocR cells (84.4 ± 1.9%) were in the $G_2$-M phase of the cell cycle after 24-hour treatment with STLC, as confirmed by the presence of cyclin B1 and phospho-$Thr_{232}$ Aurora B (Fig. 3A and Supplementary Fig. S2). As for LNCaP, LDocR cells then proceeded to apoptosis, as indicated by the increase in the proportion of cells with a sub-$G_1$ DNA content from 6.9% (±2.9%) at 48 hours to 14.9% (±2.5%) at 72 hours and the accompanying cleavage of PARP, caspase-3, and caspase-7. Comparison of the $G_2$-M and sub-$G_1$ DNA contents in LNCaP and LDocR cells following STLC treatment at 48 and 72 hours revealed very similar profiles (Figs. 2A and 3A and B). Therefore, the development of docetaxel resistance in LDocR cells has not affected the sensitivity to STLC.

PDocR cells (docetaxel-resistant derivatives of PC3M) were also tested for sensitivity to STLC. The $GI_{50}$ of STLC in PDocR cells was approximately 820 nmol/L,

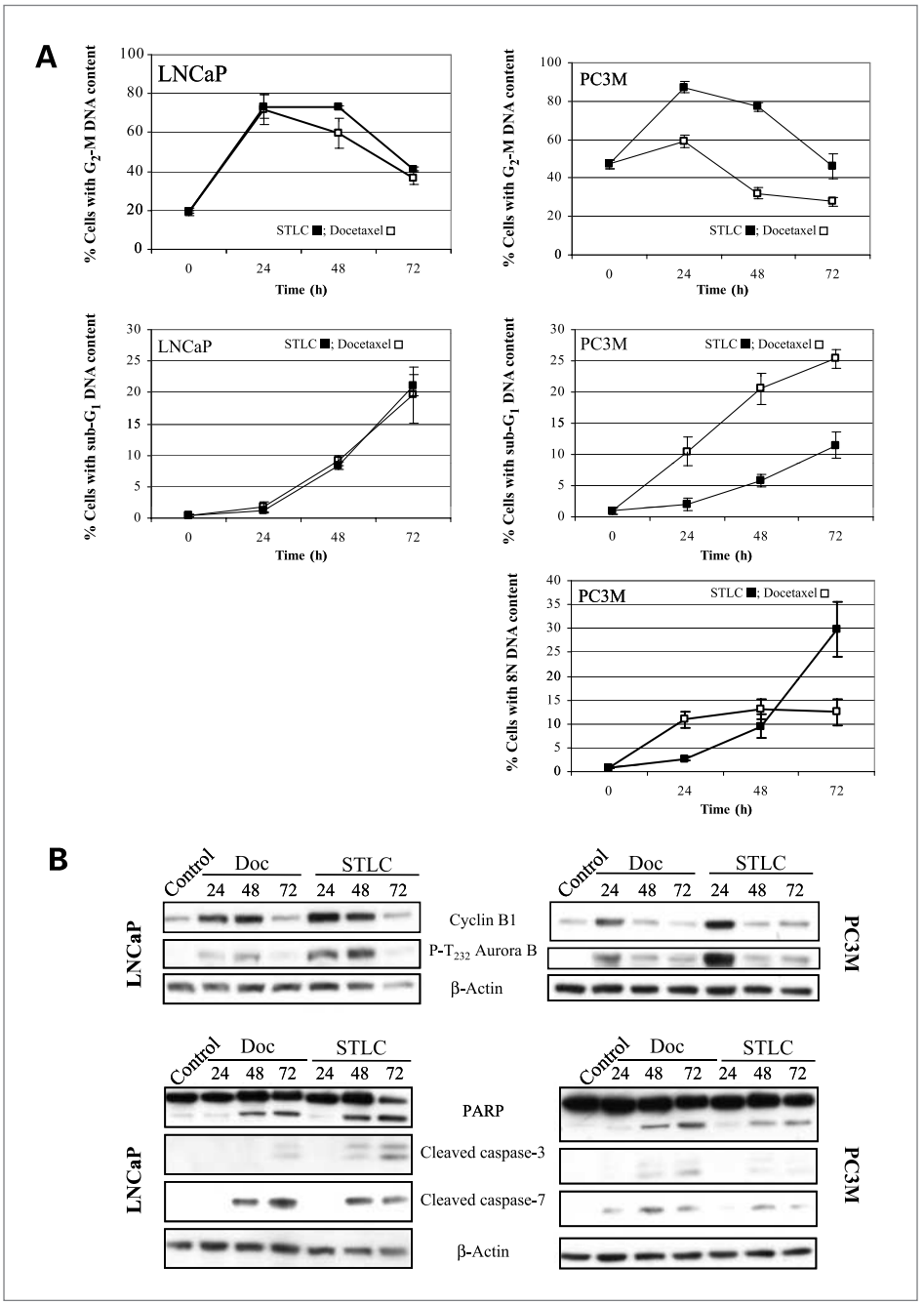


**Figure 2.** PI profiles of LNCaP and PC3M cells following STLC or docetaxel treatment. A, quantification of PI-stained cells with $G_2$-M and sub-$G_1$ DNA content over 72-h treatment with STLC (■) or docetaxel (□); the respective doses are detailed in Materials and Methods (under subheading of cell cycle profiling) and in Supplementary Fig. S1A. For PC3M cells, additional data for quantification of PI-stained cells with 8N DNA content are included. B, Western blots of matched protein samples for cell cycle–regulated proteins and apoptotic markers.

Downloaded from http://aacrjournals.org/mct/article-pdf/9/6/1730/1888559/1730.pdf by guest on 20 September 2024

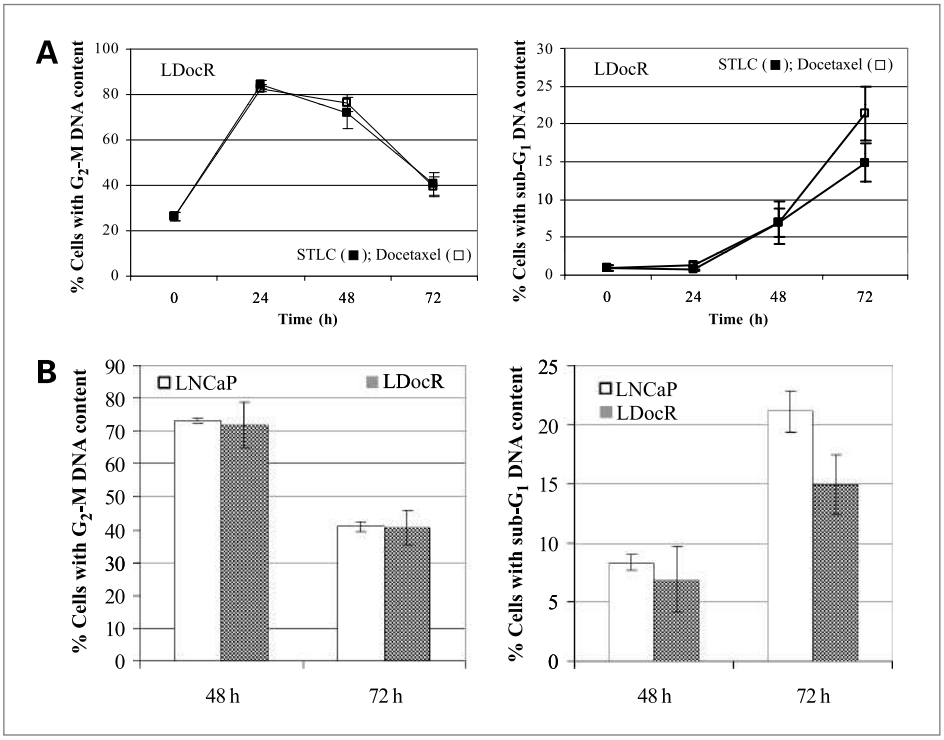


Figure 3. LNCaP docetaxel-resistant (LDocR) cells are still sensitive to the effects of STLC. A, quantification of LDocR cells with $G_2$-M and sub-$G_1$ DNA content after treatment with 2 μmol/L STLC (■) and 20 nmol/L docetaxel (□). B, comparison of the quantified PI-stained $G_2$-M and sub-$G_1$ populations of LNCaP (open columns) and LDocR cells (filled columns) in response to 1 and 2 μmol/L STLC, respectively [*P* values do not reach statistical significance (95% confidence)].

very similar to that of PC3M (Table 1). The inhibition of cell growth was initially accounted for by an increase in cells in the $G_2$-M portion of the cell cycle (up to 90.7% in the first 24 hours), with induction of cyclin B1 and phospho-$Thr_{232}$ Aurora B (Fig. 4A and Supplementary Fig. S2). Thereafter, a significant proportion of cells became polyploid, assessed as cells with an 8N DNA content, whereas only a very small proportion (≤2%) of cells underwent apoptosis (Fig. 4A and B). Statistical analysis indicated that the $G_2$-M population at 72 hours and the sub-$G_1$ populations at 48 and 72 hours differed significantly between PC3M and PDocR ($P = 0.025$, $P = 0.010$, and $P = 0.013$, respectively). The difference between the $G_2$-M populations at 48 hours was highly significant ($P = 0.007$; Fig. 4C). Although not statistically significant, PC3M cells, when compared with PDocR cells, tend to have a slightly higher proportion of polyploid population following STLC treatment. Compared with the parental PC3M cells, PDocR cells had a relatively prolonged $G_2$-M arrest and reduced induction of apoptosis (Fig. 4C).

PDocR and LDocR cells have a number of potential mechanisms of resistance to docetaxel. Both cells lines have increased expression and activity of the ABC transporter MDR1 (or ABCB1) as well as altered β-tubulin expression (with both DocR cell lines showing significant downregulation in the expression of class II and class III β-tubulins). Of note, the MDR1 expression was upregulated by 8.8- and 11-fold in LDocR and PDocR cells, respectively, relative to their parental cell lines.[5] The activity of the MDR1 transporter was also significantly higher in DocR cells when compared with their parental counterparts at 37°C ($P = 0.05$ and $P = 0.0003$, LDocR and PDocR cells, respectively; Fig. 5A and B). In LDocR and PDocR cells, there was a significantly increased efflux of rhodamine 123 at 37°C, when compared with efflux at the biologically inactive temperature of 4°C ($P = 0.007$ and $P = 0.0001$, respectively). This was reversed by the addition of the MDR1-specific inhibitor verapamil hydrochloride ($P = 0.01$ and $P = 0.007$, respectively; Fig. 5). Hence, the effects of STLC observed in docetaxel-resistant prostate cancer cells were shown to be independent of the MDR1 status.

In summary, our data on STLC as a novel Eg5 inhibitor in prostate cancer revealed its usefulness to be independent of both p53 status and sensitivity to taxane-related therapy. This highlights the importance of more detailed knowledge of the molecular mechanism regulating the polyploidy checkpoint, including the role of p53 in ongoing development of target therapy against mitotic spindle proteins.

## Discussion

Eg5 can be considered an attractive target for therapy in cancer: (*a*) Eg5 plays an essential role in mitotic progression; (*b*) beneficial effects of *in vitro* suppression Eg5 function/expression have been suggested in a number of tumor types including breast, lung, colon, ovary, and now prostate cancer; (*c*) taxane-based therapy is

[5] J. Stockley, C.N. Robson, and H.Y. Leung, unpublished data.

Downloaded from http://aacrjournals.org/mct/article-pdf/9/6/1730/1888559/1730.pdf by guest on 20 September 2024

associated with a significant toxicity profile; and (*d*) a significant proportion of tumors have intrinsic or acquired resistance to taxane-based therapy. Most described Eg5 inhibitors act by a novel mechanism of action compared with microtubule-targeting agents. They are uncompetitive with respect to ATP and act as allosteric inhibitors by binding to a pocket distant to the ATP binding pocket. They contrast to ATP-competitive kinase inhibitors that bind to the conserved nucleotide-binding pocket, provoking specificity issues.

Our main findings are that STLC remains effective in docetaxel-resistant cells and its effects are not affected by the level of upregulated P-glycoprotein function observed in our prostate cancer cell model. Although our cell-based data revealed interesting and potentially important differences among human prostate cancer cells

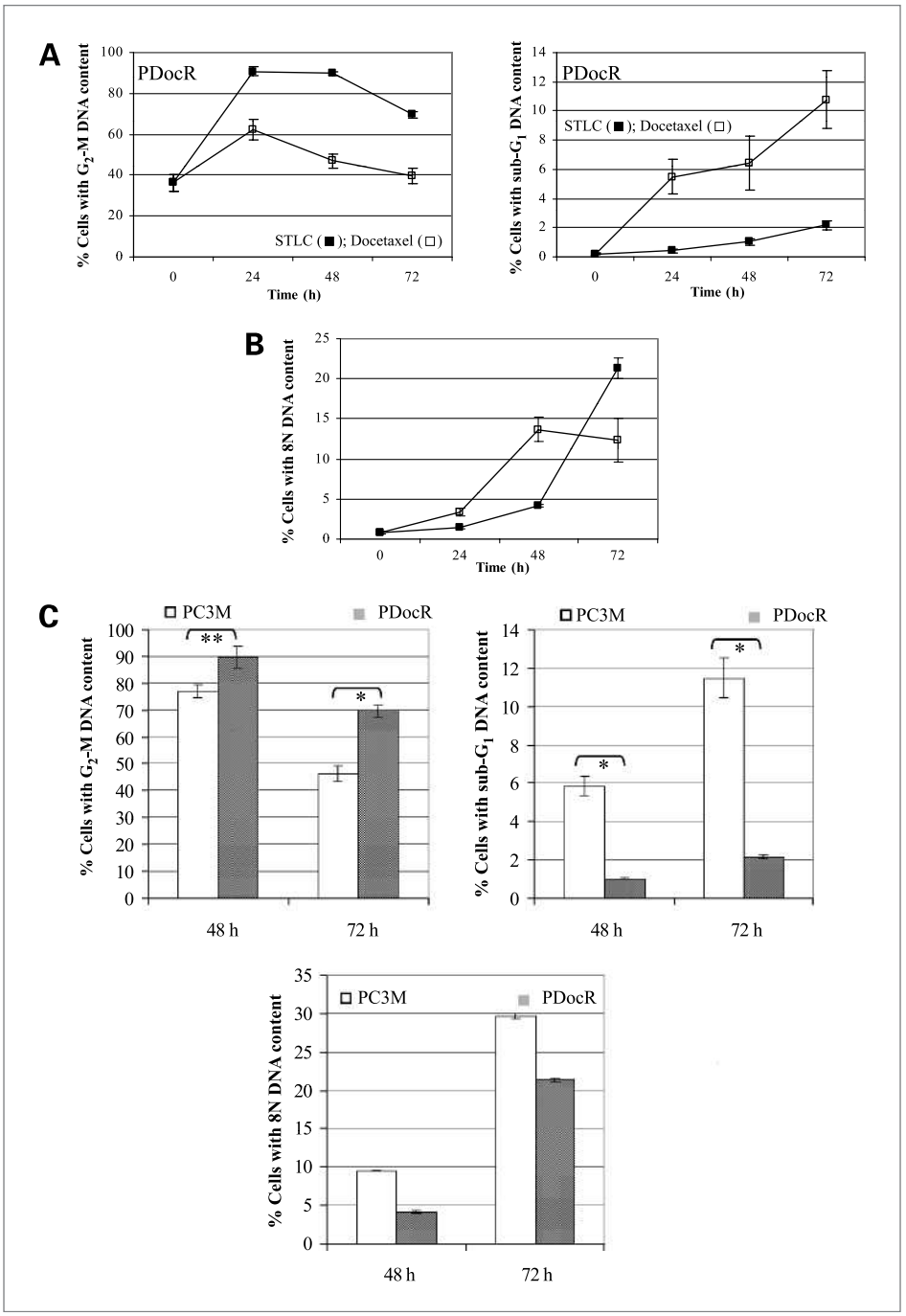


**Figure 4.** PC3M docetaxel-resistant (PDocR) cells are still sensitive to the effects of STLC. A, quantification of PDocR cells with $G_2$-M and sub-$G_1$ DNA content after treatment with 5 μmol/L STLC (■) and 20 nmol/L docetaxel (□). B, quantification of PI-stained PC3M with 8N DNA content after treatment with 5 μmol/L STLC (■) and 20 nmol/L docetaxel (□). C, comparison of the quantified PI-stained $G_2$-M, sub-$G_1$, and 8N populations of PC3M (open columns) and PDocR (filled columns) in response to 5 μmol/L STLC (*, $P < 0.05$; **, $P < 0.01$).

Downloaded from http://aacrjournals.org/mct/article-pdf/9/6/1730/1888559/1730.pdf by guest on 20 September 2024

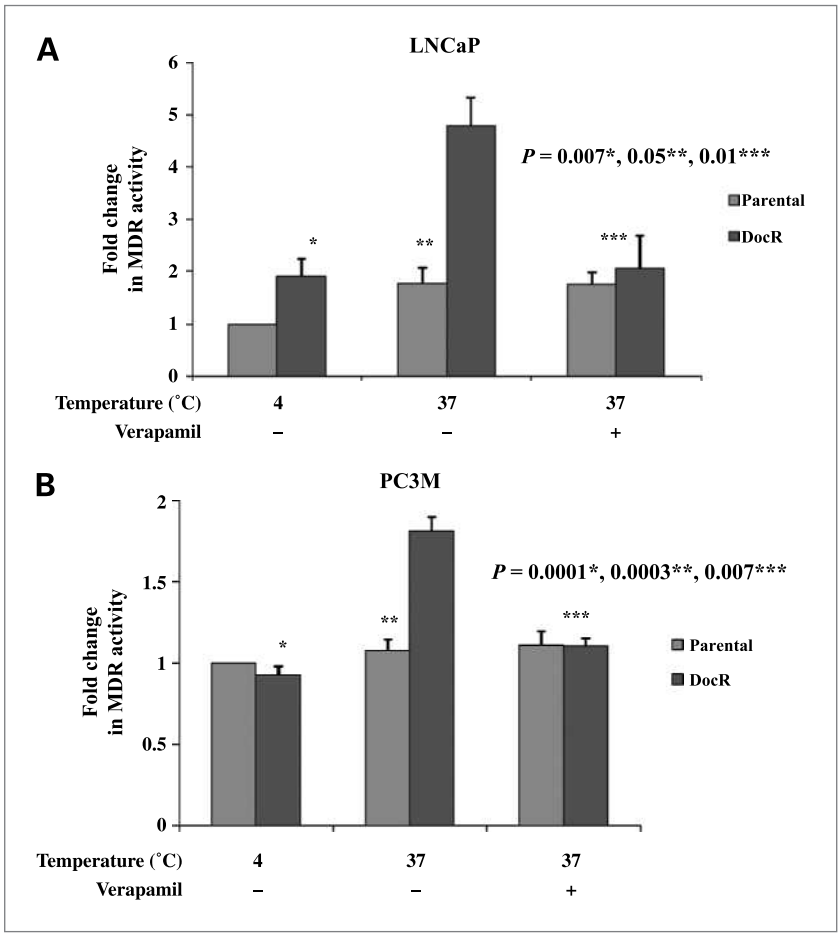


Figure 5. MDR1 activity is upregulated in docetaxel-resistant LNCaP- and PC3M-derived cells. MDR1 function was assessed by efflux of rhodamine 123 using a Becton Dickinson FACScan, and data were normalized to controls at 4°C. Verapamil hydrochloride was used as an inhibitor of the P-glycoprotein efflux pump.

in their response to STLC (and docetaxel), it is prudent to note the genetic heterogeneity between LNCaP cells (p53 wild-type and androgen receptor positive) and PC3M cells (p53 deficient and androgen receptor negative); hence, future mechanistic analysis on isogenic cell lines is warranted. Two systematic analyses on the single-cell level showed that the duration of the mitotic arrest does not necessarily dictate the cell fate (cell death or not) following inhibition of Eg5 function (18, 19). Consistent with these reports, we identified close correlation between caspase activities and cell death as indicated by the sub-$G_1$ population. Gascoigne and Taylor (19) further hypothesized that the cell fate following Eg5 inhibition is dictated by two competing but independent mechanisms, namely, caspase activation and the protection of cyclin B1 from degradation (19). However, although we observed clear evidence of cyclin B1 degradation in PC3M and PDocR cells following STLC treatment, caspase-mediated apoptosis was not induced, suggesting that additional molecular factor(s) may be at work. Despite having similar $GI_{50}$ values, PDocR cells have enhanced $G_2$-M arrest and reduced sub-$G_1$ populations when compared with the parental PC3M cells. It will therefore be important to use isogenic cell lines such as PC3M and PDocR to investigate the effects of manipulating caspase activation and/or cyclin B1 on cell fate (death or survival). In addition, novel factors may also be identified.

Docetaxel treatment in DocR cells was used at 20 nmol/L, approximately at the respective $GI_{50}$s, and would expect to have significant cellular effects, including induction of apoptosis. The $GI_{50}$ of docetaxel for the parental LNCaP cells was <2 nmol/L, ~14-fold lower than that for LDocR cells (22.4 nmol/L; detailed in Materials and Methods). Interestingly, other PC3-derived docetaxel-resistant cell lines have been reported with widely varying degrees of resistance. The reported resistance factor ranged from 4 to 400 nmol/L (20). The LDocR cells used in our report therefore represent a moderately resistant derived cell line, with just a >10-fold increase in the $GI_{50}$ value for docetaxel along with increased MDR1 activity (Fig. 5). The choice of docetaxel dose at 10 to 20 nmol/L for LNCaP and PC3M cells was based on an equipotent dose of docetaxel, which would produce a similar level of growth inhibition to that used in STLC growth assay (~$GI_{80}$).

Both adherent and floating cells were collected for cell cycle profiling and Western blotting. Hence, the data from

Downloaded from http://aacrjournals.org/mct/article-pdf/9/6/1730/1888559/1730.pdf by guest on 20 September 2024

cell cycle analysis will reflect the overall cellular response, including both viable and dead cells, regardless of their mitotic state. The proportion of nonviable cells is represented in the sub-$G_1$ phase of individual data sets. The data obtained from fluorescence-activated cell sorting (FACS) are representative of the overall cellular condition. Consistent with our data, in a recent report using antisense oligonucleotide to target Eg5, LNCaP cells were also found to be more sensitive to Eg5-targeted treatment than PC3 cells. The authors attributed this difference to the relatively lower expression level of Eg5 in LNCaP cells in their report (21). However, based on our data and others, it is likely that differences seen between LNCaP and PC3M cells in their response to STLC are related to distinct molecular mechanisms rather than a consequence of the minor difference in their respective Eg5 expression levels. Furthermore, the doubling time of each of the cell lines studied does not vary significantly (Supplementary Table) and is not expected to account for the observed differences. The data obtained at 72 hours would represent between 2.6 and 3 doublings for all the cell lines studied. It is worth noting that the docetaxel-resistant cell lines have relatively short doubling times. Studying the cellular response of LNCaP and LDocR to STLC treatment for an extended period (up to 5 days), we observed a progressive increase in proportion of cells in the sub-$G_1$ phase, signifying cell death: LNCaP—3 days (72 hours), 20%; 4 days, 36%; 5 days, 46%; LDocR—3 days (72 h), 15%; 4 days, 52%; 5 days, 53% (data not shown).

To date, to our knowledge, seven Eg5 inhibitors have entered clinical phase I or phase II trials. Except for MK-0731 (Merck), which is now inactive, their preclinical and clinical evaluations are currently under way. Preliminary results are encouraging with potential improvement in side effect profiles when compared with tubulin-targeting drugs, and in certain cases, partial responses have been reported (22). One of the first Eg5 inhibitors reported, ispinesib, has been assessed in a phase II study in "androgen-independent" prostate cancer (23). In this report, no efficacy was observed; however, neither were any monopolar spindles observed in control peripheral blood monocytes obtained from treated patients. This suggests a lack of efficacy against the target of interest, namely, Eg5. More potent inhibitors against Eg5 with better drug-like properties may enhance the efficacy as well as reduce any off-target toxicities (23).

A number of biologically distinct processes can result in a reduction in cell proliferation. In HeLa cells, STLC suppresses cell proliferation by induction of transient arrest in the $G_2$-M phase of the cell cycle, followed by subsequent apoptosis (7, 8). STLC-treated PC3M cells underwent a transient $G_2$-M arrest, followed by polyploidy, whereas docetaxel-treated PC3M cells proceeded to apoptosis after a transient $G_2$-M arrest. Lanzi et al. reported that, following treatment with paclitaxel, DU145 cells (with mutated p53) underwent arrest in $G_2$-M followed by apoptosis, whereas PC3 underwent mitotic slippage and subsequently became polyploidy (14). However, the fate of the polyploidy PC3M cells is unknown. Principally, polyploidy cells can either die in the tetraploid state (senesce) or continue to divide (18, 19). As previously mentioned, PC3 cells undergo a transient mitotic arrest followed by the development of polyploidy when treated with paclitaxel (14). These polyploid cells were found to undergo a slow and delayed death after the process of endo-reduplication. In addition, Eg5 inhibition by a number of methods has been reported to preferentially kill tetraploid human colon carcinoma (24). The importance of sequential activation of the spindle assembly checkpoint followed by mitotic slippage has been suggested for the induction of apoptosis by the Eg5 inhibitor KSP-1A (25). Although this is consistent with our data, the presence of mitotic arrest before the induction of apoptosis may not be necessary (17).

Marcus et al. (26) previously reported that docetaxel-resistant PC3 cells remained sensitive to the effects of Eg5 inhibition by the use of an antisense oligonucleotide (26). Interestingly, a large proportion of both these cells and the parental PC3 cells still underwent apoptosis in response to Eg5 inhibition at a high dose of oligonucleotide, unlike the PC3M parental and PDocR cells in our hands. This may represent off-target effects or nonspecific toxicity due to high concentration of transfected antisense oligonucleotide.

STLC is highly specific to Eg5, and therefore the mechanism of action between parental and their respective docetaxel-resistant cells is expected to be the same. There is, however, a key difference in the cell fate, particularly between PC3M and PDocR cells, namely, whether individual cells proceed to cell death or cell cycle arrest or eventually successfully return to cell cycle. Taken together, our *in vitro* data support the consideration of Eg5 as a potential therapeutic target in prostate cancer. Future efforts will focus on the *in vivo* assessment of STLC and related analogues in prostate cancer either alone or in combination with other drugs.

## Disclosure of Potential Conflicts of Interest

No potential conflicts of interest were disclosed.

## Acknowledgments

We thank Professor Dave Gillespie for helpful comments and discussions.

## Grant Support

Cancer Research UK and Glasgow Royal Infirmary Endowment Fund. Image acquisition system following immunohistochemistry experiment was in part funded by a grant from Think Pink Charity, UK. C. Wiltshire and B.L. Singh are funded by the Glasgow Royal Infirmary Endowment and the Astella Foundation, respectively; J. Fleming, B. Doyle, F. Kozielski, and H.Y. Leung receive research support from Beatson Institute for Cancer Research (Cancer Research UK).

The costs of publication of this article were defrayed in part by the payment of page charges. This article must therefore be hereby marked *advertisement* in accordance with 18 U.S.C. Section 1734 solely to indicate this fact.

Received 12/07/2009; revised 03/11/2010; accepted 04/12/2010; published OnlineFirst 06/01/2010.

Downloaded from http://aacrjournals.org/mct/article-pdf/9/6/1730/1888559/1730.pdf by guest on 20 September 2024

## References


1. Hirokawa N, Noda Y. Intracellular transport and kinesin superfamily proteins, KIFs: structure, function, and dynamics. Physiol Rev 2008; 88:1089–118.
2. Zhu C, Zhao J, Bibikova M, et al. Functional analysis of human microtubule-based motor proteins, the kinesins and dyneins, in mitosis/cytokinesis using RNA interference. Mol Biol Cell 2005;16: 3187–99.
3. Blangy A, Lane HA, d'Herin P, Harper M, Kress M, Nigg EA. Phosphorylation by p34cdc2 regulates spindle association of human Eg5, a kinesin-related motor essential for bipolar spindle formation *in vivo*. Cell 1995;83:1159–69.
4. Mayer TU, Kapoor TM, Haggarty SJ, King RW, Schreiber SL, Mitchison TJ. Small molecule inhibitor of mitotic spindle bipolarity identified in a phenotype-based screen. Science 1999;286:971–4.
5. Bergnes G, Brejc K, Belmont L. Mitotic kinesins: prospects for antimitotic drug discovery. Curr Top Med Chem 2005;5:127–45.
6. DeBonis S, Skoufias DA, Lebeau L, et al. *In vitro* screening for inhibitors of the human mitotic kinesin Eg5 with antimitotic and antitumor activities. Mol Cancer Ther 2004;3:1079–90.
7. Skoufias DA, DeBonis S, Saoudi Y, et al. *S*-Trityl-L-cysteine is a reversible, tight binding inhibitor of the human kinesin Eg5 that specifically blocks mitotic progression. J Biol Chem 2006;281:17559–69.
8. Kozielski F, Skoufias DA, Indorato RL, et al. Proteome analysis of apoptosis signaling by *S*-trityl-L-cysteine, a potent reversible inhibitor of human mitotic kinesin Eg5. Proteomics 2008;8:289–300.
9. Ogo N, Oishi S, Matsuno K, Sawada J, Fujii N, Asai A. Synthesis and biological evaluation of L-cysteine derivatives as mitotic kinesin Eg5 inhibitors. Bioorg Med Chem Lett 2007;17:3921–4.
10. Debonis S, Skoufias DA, Indorato RL, et al. Structure-activity relationship of *S*-trityl-L-cysteine analogues as inhibitors of the human mitotic kinesin Eg5. J Med Chem 2008;51:1115–25.
11. Figg WD, Walls RG, Cooper MR, et al. *In vitro* antitumor effect of hydroxyurea on hormone-refractory prostate cancer cells and its potentiation by phenylbutyrate. Anticancer Drugs 1994;5:336–42.
12. McCracken SR, Ramsay A, Heer R, et al. Aberrant expression of extracellular signal-regulated kinase 5 in human prostate cancer. Oncogene 2008;27:2978–88.
13. Lee JS, Paull K, Alvarez M, et al. Rhodamine efflux patterns predict P-glycoprotein substrates in the National Cancer Institute drug screen. Mol Pharmacol 1994;46:627–38.
14. Lanzi C, Cassinelli G, Cuccuru G, et al. Cell cycle checkpoint efficiency and cellular response to paclitaxel in prostate cancer cells. Prostate 2001;48:254–64.
15. Carroll AG, Voeller HJ, Sugars L, Gelmann EP. p53 oncogene mutations in three human prostate cancer cell lines. Prostate 1993; 23:123–34.
16. Lanni JS, Jacks T. Characterization of the p53-dependent postmitotic checkpoint following spindle disruption. Mol Cell Biol 1998; 18:1055–64.
17. Tsuiki H, Nitta M, Tada M, Inagaki M, Ushio Y, Saya H. Mechanism of hyperploid cell formation induced by microtubule inhibiting drug in glioma cell lines. Oncogene 2001;20:420–9.
18. Shi J, Orth JD, Mitchison T. Cell type variation in responses to antimitotic drugs that target microtubules and kinesin-5. Cancer Res 2008;68:3269–76.
19. Gascoigne KE, Taylor SS. Cancer cells display profound intra- and interline variation following prolonged exposure to antimitotic drugs. Cancer Cell 2008;14:111–22.
20. Lo Nigro C, Maffi M, Fischel JL, Formento P, Milano G, Merlano M. The combination of docetaxel and the somatostatin analogue lanreotide on androgen-independent docetaxel-resistant prostate cancer: experimental data. BJU Int 2008;102:622–7.
21. Hayashi N, Koller E, Fazli L, Gleave ME. Effects of Eg5 knockdown on human prostate cancer xenograft growth and chemosensitivity. Prostate 2008;68:1283–95.
22. Huszar D, Theoclitou ME, Skolnik J, Herbst R. Kinesin motor proteins as targets for cancer therapy. Cancer Metastasis Rev 2009; 28:197–208.
23. Beer TM, Goldman B, Synold TW, et al. Southwest Oncology Group phase II study of ispinesib in androgen-independent prostate cancer previously treated with taxanes. Clin Genitourin Cancer 2008;6:103–9.
24. Rello-Varona S, Vitale I, Kepp O, et al. Preferential killing of tetraploid tumor cells by targeting the mitotic kinesin Eg5. Cell Cycle 2009; 8:1030–5.
25. Tao W, South VJ, Zhang Y, et al. Induction of apoptosis by an inhibitor of the mitotic kinesin KSP requires both activation of the spindle assembly checkpoint and mitotic slippage. Cancer Cell 2005;8:49–59.
26. Marcus AI, Peters U, Thomas SL, et al. Mitotic kinesin inhibitors induce mitotic arrest and cell death in Taxol-resistant and -sensitive cancer cells. J Biol Chem 2005;280:11569–77.


Downloaded from http://aacrjournals.org/mct/article-pdf/9/6/1730/1888559/1730.pdf by guest on 20 September 2024